2005 International Linear Collider Workshop - Stanford, U.S.A.

The MSSM Higgs Sector at $\mathcal{O}(\alpha_b\alpha_s)$ and Beyond

S. Heinemeyer
CERN TH Division, Department of Physics, CH-1211 Geneva 23, Switzerland
W. Hollik, H. Rzehak
Max-Planck-Institut für Physik (Werner-Heisenberg-Institut), Föhringer Ring 6, D–80805 Munich, Germany
G. Weiglein
Institute for Particle Physics Phenomenology, University of Durham, Durham DH1 3LE, UK

arXiv:hep-ph/0506254v1 24 Jun 2005

We evaluate $\mathcal{O}(\alpha_b\alpha_s)$ corrections in the MSSM Higgs boson sector, including an analysis of the renormalization in the bottom/scalar bottom sector. For $\mu < 0$ the genuine two-loop corrections to the mass of the lightest Higgs boson mass can amount up to 3 GeV. Different renormalization schemes are applied and numerically compared. Likewise the residual dependence on the renormalization scale is investigated. This allows to determine the remaining theoretical uncertainties from unknown higher-order corrections at $\mathcal{O}(\alpha_b\alpha_s^2)$ for different regions of the MSSM parameter space.

1. INTRODUCTION

A crucial prediction of the Minimal Supersymmetric Standard Model (MSSM) [1] is the existence of at least one light Higgs boson. Direct searches at LEP have already ruled out a considerable fraction of the MSSM parameter space [2, 3], and the forthcoming high-energy experiments at the Tevatron, the LHC, and the International Linear Collider (ILC) will either discover a light Higgs boson or rule out Supersymmetry (SUSY) as a viable theory for physics at the weak scale. Furthermore, if one or more Higgs bosons are discovered, bounds on their masses and couplings will be set at the LHC [4, 5]. Eventually the masses and couplings will be determined with high accuracy at the ILC [6–8]. Thus, a precise knowledge of the dependence of masses and mixing angles in the MSSM Higgs sector on the relevant supersymmetric parameters is of utmost importance to reliably compare the predictions of the MSSM with the (present and future) experimental results. Even nowadays a precise prediction of the lightest MSSM Higgs boson mass is important to set solid bounds on the MSSM parameter space [9, 10].

The status of the available results for the higher-order contributions to the neutral $\mathcal{CP}$-even MSSM Higgs boson masses has been summarized in Refs. [11–13]. In particular two-loop contributions to the leading one-loop corrections involving the top and bottom Yukawa couplings (with $\alpha_t \equiv h_t^2/(4\pi)$, $\alpha_b \equiv h_b^2/(4\pi)$, $h_{t,b}$ being the superpotential top or bottom coupling) have been evaluated. Corrections from the bottom/sbottom sector can also give large effects, in particular for large values of $\tan\beta$, the ratio of the two vacuum expectation values, $\tan\beta = v_2/v_1$, and large values of μ, the supersymmetric Higgs mass parameter. The leading strong corrections at $\mathcal{O}(\alpha_b\alpha_s)$ have been derived in Ref. [14] (in the limit $\tan\beta \to \infty$) and in Ref. [15] (for arbitrary $\tan\beta$). In the (s)bottom corrections the all-order resummation of the $\tan\beta$-enhanced terms, $\mathcal{O}(\alpha_b(\alpha_s\tan\beta)^n)$, is also performed [16, 17]. Furthermore a full effective potential two-loop calculation exists [18], however, no public code is available.

The potentially large size of corrections from the $b/\tilde{b}$ sector makes it desirable to investigate the corresponding two-loop corrections, including the applied renormalization. An inconvenient scheme can give rise to artificially large corrections, whereas a convenient scheme absorbs the dominant contributions into the one-loop result, and higher-order corrections remain small. The comparison of different schemes (without artificially enhanced corrections) and the renormalization scheme dependence give an indication of the possible size of missing higher-order terms of $\mathcal{O}(\alpha_b\alpha_s^2)$.

2. THE MSSM HIGGS SECTOR AND RENORMALIZATION

The Higgs sector of the MSSM [19] comprises two neutral $\mathcal{CP}$-even Higgs bosons, h and H ($m_h < m_H$), the $\mathcal{CP}$-odd A boson (throughout this paper we assume that $\mathcal{CP}$ is conserved) and two charged Higgs bosons, $H^\pm$.

In the Feynman-diagrammatic (FD) approach, the higher-order corrected Higgs boson masses, M_h and M_H, are derived as the poles of the h, H-propagator matrix, i.e. by solving the equation

$$\left[p^2 - m^2_{h,\rm tree} + \hat{\Sigma}_{hh}(p^2)\right]\left[p^2 - m^2_{H,\rm tree} + \hat{\Sigma}_{HH}(p^2)\right] - \left[\hat{\Sigma}_{hH}(p^2)\right]^2 = 0\,. \tag{1}$$

The renormalized self-energies, $\hat{\Sigma}_s$, can be expanded according to the one-, two-, ... loop-order contributions,

$$\hat{\Sigma}_s(p^2) = \hat{\Sigma}^{(1)}_s(p^2) + \hat{\Sigma}^{(2)}_s(p^2) + \cdots\,, s = hh, hH, HH\ . \tag{2}$$

The leading two-loop corrections from the $b/\tilde{b}$ sector are the $\mathcal{O}(\alpha_s)$ corrections to the dominant one-loop contributions of $\mathcal{O}(\alpha_b)$. They are obtained for zero external momentum and neglecting the gauge couplings, see Ref. [15] for further details. This approach is analogous to the way the leading one- and two-loop contributions in the top/stop sector have been obtained (see e.g. Ref. [20]). Details about the renormalization in the MSSM Higgs sector can be found in Ref. [15].

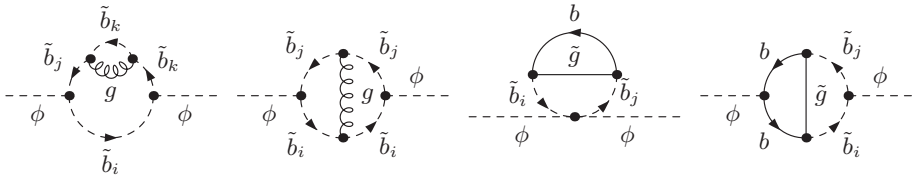

Figure 1: Some generic two-loop diagrams for the Higgs-boson self-energies ($\phi = h, H, A$; $i, j, k, l = 1, 2$). Similar diagrams arise for the tadpole contributions.

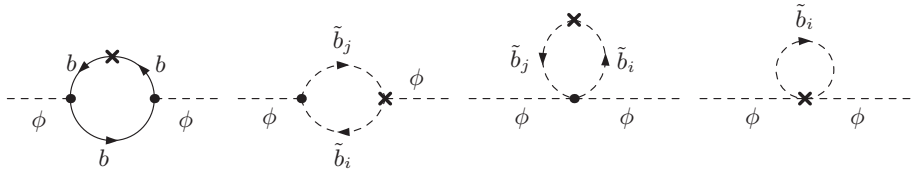

Figure 2: Some generic one-loop diagrams with counterterm insertion for the Higgs-boson self-energies ($\phi = h, H, A$), $i, j, k = 1, 2$). Similar diagrams arise for the tadpole contributions.

The genuine two-loop Feynman diagrams to be evaluated for the Higgs boson self-energies, $\hat{\Sigma}_{hh,hH,HH}$, are shown in Fig. 1. The diagrams with subloop renormalization are depicted in Fig. 2. The diagrams and the corresponding amplitudes have been generated with the package *FeynArts* [21, 22]. The further evaluation has been done using the program *TwoCalc* [23].

We now turn to the renormalization in the scalar-quark sector, entering via the diagrams depicted in Fig. 2. Since the two-loop self-energies are evaluated at $\mathcal{O}(\alpha_{t,b}\alpha_s)$ it is sufficient to determine the counterterms induced by the strong interaction only. The tree-level relations and further details about our notation can be found in Ref. [15]. In the following $m_{\tilde{q}_i}$, $i = 1, 2$ denotes the two mass eigenvalues of the stop ($q = t$) and sbottom ($q = b$) sector. The corresponding unitary diagonalization matrix is denoted as $U_{\tilde{q}_{ij}}$, $i, j = 1, 2$.

2.1. Renormalization of the top and scalar-top sector

The $t/\tilde{t}$ sector contains four independent parameters: the top-quark mass m_t, the stop masses $m_{\tilde{t}_1}$ and $m_{\tilde{t}_2}$, and either the squark mixing angle $\theta_{\tilde{t}}$ or, equivalently, the trilinear coupling A_t. Accordingly, the renormalization of

this sector is performed by introducing four counterterms that are determined by four independent renormalization conditions. The following renormalization conditions are imposed (see also Ref. [24]).

(i) On-shell renormalization of the top-quark mass

(ii) On-shell renormalization of the stop masses

(iii) The counterterm for the mixing angle, $\theta_{\tilde{t}}$: $\delta\theta_{\tilde{t}} = \left[\mathrm{Re}\,\Sigma_{\tilde{t}_{12}}(m^2_{\tilde{t}_1}) + \mathrm{Re}\,\Sigma_{\tilde{t}_{12}}(m^2_{\tilde{t}_2})\right] / \left[2(m^2_{\tilde{t}_1} - m^2_{\tilde{t}_2})\right]$.

Having already specified $\delta\theta_{\tilde{t}}$, the A_t counterterm cannot be defined independently but follows from the relation $\sin 2\theta_{\tilde{t}} = [2m_t(A_t - \mu\cot\beta)]\,/[m^2_{\tilde{t}_1} - m^2_{\tilde{t}_2}]$.

2.2. Renormalization of the bottom and scalar-bottom sector

Because of $SU(2)$-invariance the soft-breaking parameters for the left-handed stops and sbottoms are identical, and thus the $\tilde{t}$ and $\tilde{b}$ masses are not independent but connected via the relation

$$\cos^2\theta_{\tilde{b}} m^2_{\tilde{b}_1} + \sin^2\theta_{\tilde{b}} m^2_{\tilde{b}_2} = \cos^2\theta_{\tilde{t}} m^2_{\tilde{t}_1} + \sin^2\theta_{\tilde{t}} m^2_{\tilde{t}_2} + m_b^2 - m_t^2 - M_W^2\cos(2\beta)\ . \tag{3}$$

Since the $\tilde{t}$ masses have already been renormalized on-shell, only one of the $\tilde{b}$ mass counterterms can be determined independently. In the following, the $\tilde{b}_2$ mass is chosen as the pole mass, yielding $\delta m^2_{\tilde{b}_2} = \mathrm{Re}\,\Sigma_{\tilde{b}_{22}}(m^2_{\tilde{b}_2})$, whereas the counterterm for $m_{\tilde{b}_1}$ is determined as a combination of other counterterms, according to

$$\begin{aligned}\delta m^2_{\tilde{b}_1} = \frac{1}{\cos^2\theta_{\tilde{b}}}\Big(&\cos^2\theta_{\tilde{t}}\delta m^2_{\tilde{t}_1} + \sin^2\theta_{\tilde{t}}\delta m^2_{\tilde{t}_2} - \sin^2\theta_{\tilde{b}}\delta m^2_{\tilde{b}_2} - \sin 2\theta_{\tilde{t}}(m^2_{\tilde{t}_1} - m^2_{\tilde{t}_2})\delta\theta_{\tilde{t}} \\ &+ \sin 2\theta_{\tilde{b}}(m^2_{\tilde{b}_1} - m^2_{\tilde{b}_2})\delta\theta_{\tilde{b}} - 2m_t\,\delta m_t + 2m_b\,\delta m_b\Big)\ .\end{aligned} \tag{4}$$

Consequently, the numerical value of $m_{\tilde{b}_1}$ does not correspond to the pole mass. The pole mass can be obtained from $m_{\tilde{b}_1}$ via a finite shift of $\mathcal{O}(\alpha_s)$ (see e.g. Ref. [25]).

There are three more parameters with counterterms to be determined: the b-quark mass m_b, the mixing angle $\theta_{\tilde{b}}$, and the trilinear coupling A_b. They are connected via

$$\sin 2\theta_{\tilde{b}} = [2m_b(A_b - \mu\tan\beta)]\,/[m^2_{\tilde{b}_1} - m^2_{\tilde{b}_2}]\,, \tag{5}$$

which reads in terms of counterterms

$$2\cos 2\theta_{\tilde{b}}\ \delta\theta_{\tilde{b}} = \sin 2\theta_{\tilde{b}}\frac{\delta m_b}{m_b} + \frac{2m_b\,\delta A_b}{m^2_{\tilde{b}_1} - m^2_{\tilde{b}_2}} - \sin 2\theta_{\tilde{b}}\frac{\delta m^2_{\tilde{b}_1} - \delta m^2_{\tilde{b}_2}}{m^2_{\tilde{b}_1} - m^2_{\tilde{b}_2}}\ . \tag{6}$$

Only two of the three counterterms, δm_b, $\delta\theta_{\tilde{b}}$, δA_b can be treated as independent, which offers a variety of choices. In the following, four different renormalization schemes, collected in Tab. I, will be investigated. Details about the four schemes can be found in Ref. [15].

Table I: Summary of the four renormalization schemes for the bottom quark/squark sector. Blank entries indicate dependent quantities. For more details see Ref. [15].

scheme	$m^2_{\tilde{b}_2}$	m_b	A_b	$\theta_{\tilde{b}}$
analogous to $t/\tilde{t}$ sector ("m_b OS")	on-shell	on-shell		on-shell
$\overline{\rm DR}$ bottom-quark mass ("m_b $\overline{\rm DR}$")	on-shell	$\overline{\rm DR}$	$\overline{\rm DR}$	
$\overline{\rm DR}$ mixing angle and A_b ("A_b, $\theta_{\tilde{b}}$ $\overline{\rm DR}$")	on-shell		$\overline{\rm DR}$	$\overline{\rm DR}$
on-shell mixing angle and A_b ("A_b, $\theta_{\tilde{b}}$ OS")	on-shell		on-shell	on-shell

2.3. Resummation in the $b/\tilde{b}$ sector

The relation between the bottom-quark mass and the Yukawa coupling h_b, which in lowest order reads $m_b = h_b v_1/\sqrt{2}$, receives radiative corrections proportional to $h_b v_2 = h_b \tan\beta\, v_1$. Thus, large $\tan\beta$-enhanced contributions can occur, which need to be properly taken into account. As shown in Refs. [16, 17] the leading terms of $\mathcal{O}(\alpha_b(\alpha_s \tan\beta)^n)$ can be resummed by using an appropriate effective bottom Yukawa coupling.

Accordingly, an effective bottom-quark mass, $m_b^{\overline{\rm DR},\rm MSSM}$, is obtained by extracting its UV-finite $\tan\beta$-enhanced contribution Δm_b (which enters through Σ_{b_S}) and writing it as $1/(1+\Delta m_b)$ into the denominator. In this way the leading powers of $(\alpha_s \tan\beta)^n$ are correctly resummed [16, 17]. This yields

$$m_b^{\overline{\rm DR},\rm MSSM}(\mu^{\overline{\rm DR}}) = [m_b^{\overline{\rm MS}}(M_Z) b^{\rm shift} + \frac{1}{2} m_b(\Sigma_{b_L}^{\rm fin}(m_b{}^2) + \Sigma_{b_R}^{\rm fin}(m_b{}^2)) + m_b\, \widetilde{\Sigma}_{b_S}^{\rm fin}(m_b^2)]/[1+\Delta m_b]\ , \tag{7}$$

where $\widetilde{\Sigma}_{b_S} \equiv \Sigma_{b_S} + \Delta m_b$ denotes the non-enhanced remainder of the scalar b-quark self-energy at $\mathcal{O}(\alpha_s)$, and $b^{\rm shift}$ is given in by $b^{\rm shift} \equiv \left[1 + \frac{\alpha_s}{\pi}\left(\frac{4}{3} - \ln\frac{(m_b^{\overline{\rm MS}})^2}{M_Z^2}\right)\right]$. The $\tan\beta$-enhanced scalar part of the b-quark self-energy, Δm_b, is given at $\mathcal{O}(\alpha_s)$ by

$$\Delta m_b = -2/(3\pi)\alpha_s \tan\beta\, \mu\, m_{\tilde{g}}\, \frac{m_{\tilde{b}_1}^2 m_{\tilde{b}_2}^2 \log(m_{\tilde{b}_2}^2/m_{\tilde{b}_1}^2) + m_{\tilde{b}_1}^2 m_{\tilde{g}}^2 \log(m_{\tilde{b}_1}^2/m_{\tilde{g}}^2) + m_{\tilde{g}}^2 m_{\tilde{b}_2}^2 \log(m_{\tilde{g}}^2/m_{\tilde{b}_2}^2)}{(m_{\tilde{b}_1}^2 - m_{\tilde{g}}^2)(m_{\tilde{g}}^2 - m_{\tilde{b}_2}^2)(m_{\tilde{b}_2}^2 - m_{\tilde{b}_1}^2)}\ . \tag{8}$$

We incorporate the effective bottom-quark mass of (7) into our one-loop results for the renormalized Higgs boson self-energies. In this way the leading effects of $\mathcal{O}(\alpha_b\alpha_s)$ are absorbed into the one-loop result. We refer to the genuine two-loop contributions, which go beyond this improved one-loop result, as "subleading $\mathcal{O}(\alpha_b\alpha_s)$ corrections" in the following.

3. NUMERICAL RESULTS

For our numerical analysis we use the following parameters (if not indicated differently): $m_t = 174.3$ GeV, $m_b^{\overline{\rm MS}} = 2.94$ GeV, $M_A = 700$ GeV, $\mu = -1000$, $\tan\beta = 50$, $M_{\rm SUSY} = 1000$ GeV, $A_f = 2M_{\rm SUSY}$, $M_2 = 2M_1 = 100$ GeV, $m_{\tilde{g}} = 1000$ GeV, $\mu^{\overline{\rm DR}} = m_t$. Large values of $\tan\beta$ and $|\mu|$ are chosen in order to illustrate possibly large effects in the $b/\tilde{b}$ sector. The inclusion of all known corrections and the current experimental central top quark mass value of $m_t = 178.0$ GeV in our analysis would yield an increase in M_h of $\mathcal{O}(8$ GeV) [11]. Therefore the mass values given in our numerical analysis should not be viewed as predictions of M_h; they are rather illustrations of the α_s-corrections to the bottom Yukawa contributions at the two-loop level.

In Ref. [15] it has been shown that the "m_b OS" scheme should be discarded. The reason for the problematic behavior of this scheme is easy to understand. The renormalization condition in the "m_b OS" scheme is a condition on the sbottom mixing angle $\theta_{\tilde{b}}$ and thus on the combination $(A_b - \mu\tan\beta)$. In parameter regions where $\mu\tan\beta$ is much larger than A_b, the counterterm δA_b receives a very large finite shift when calculated from the counterterm $\delta\theta_{\tilde{b}}$. This problem is avoided in the other renormalization schemes introduced in Tab. I, where the renormalization condition is applied directly to A_b, rather than deriving δA_b from the renormalization of the mixing angle.

In Fig. 3 it can be seen that the behavior of the subleading corrections in the three remaining renormalization schemes strongly depends on the choice of $m_{\tilde{g}}$. For $m_{\tilde{g}} \lesssim 1000$ GeV all schemes lead to an increase of M_h from the subleading $\mathcal{O}(\alpha_b\alpha_s)$ corrections. For $m_{\tilde{g}} \gtrsim 1500$ GeV, on the other hand, all schemes lead to a decrease, where the size of the individual corrections also strongly varies with $m_{\tilde{g}}$. Accordingly, the relative size of the corrections in the different schemes also varies with $m_{\tilde{g}}$. Corrections up to about 3 GeV are possible. The differences between the three schemes are of $\mathcal{O}(2$ GeV) for large $m_{\tilde{g}}$. It should be noted that the effects of the higher-order corrections to M_h do not decouple with large $m_{\tilde{g}}$. The corrections at $\mathcal{O}(\alpha_t\alpha_s)$ [20] as well as $\mathcal{O}(\alpha_b\alpha_s)$ grow logarithmically in the renormalization schemes that we have adopted.

The $\mu^{\overline{\rm DR}}$ variation is shown in Fig. 4. The leading contribution (the $\mathcal{O}(\alpha_t\alpha_s)$ result including resummation) is shown as the dark shaded (black) band. The results including the subleading corrections in the "m_b $\overline{\rm DR}$" scheme are

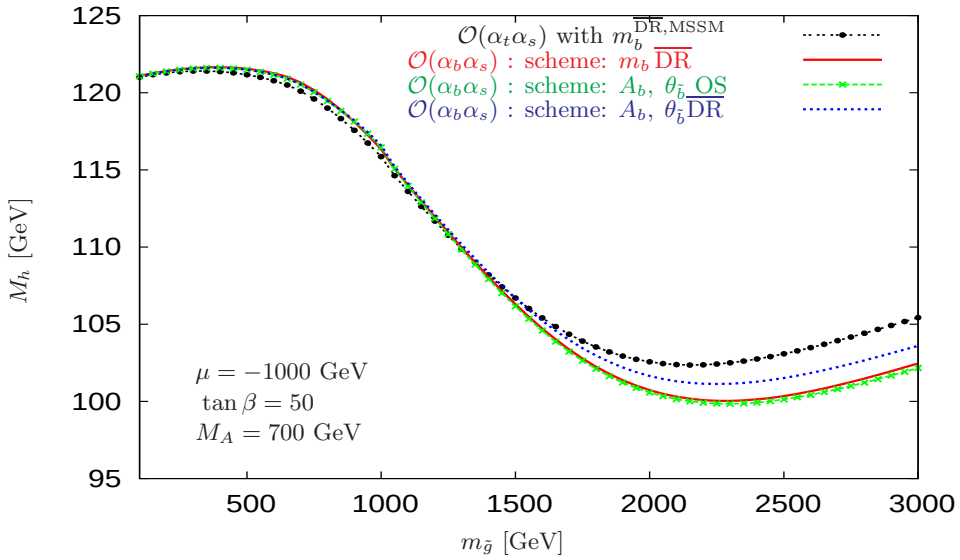

Figure 3: M_h as a function of $m_{\tilde g}$.

shown as a light shaded (red) band. It can be seen that the variation with $\mu^{\overline{\rm DR}}$ is strongly reduced by the inclusion of the subleading contributions. The variation with $\mu^{\overline{\rm DR}}$ within the "$m_b\,\overline{\rm DR}$" scheme is tiny for $m_{\tilde g} \lesssim 500$ GeV, and reaches ± 2 GeV for large $m_{\tilde g}$ values. Thus, the $\mu^{\overline{\rm DR}}$ variation causes a similar shift in M_h as the comparison between the three renormalization schemes discussed above.

The comparison of the results in the different schemes that we have analyzed and the investigation of the renormalization scale dependence give an indication of the possible size of missing higher-order corrections in the $b/\tilde b$ sector. For $\mu > 0$ (see Ref. [15]) the higher-order corrections from the $b/\tilde b$ sector (beyond $\mathcal{O}(\alpha_b\alpha_s)$) appear to be sufficiently well under control. For $\mu < 0$, on the other hand, sizable higher-order corrections from the $b/\tilde b$ sector are possible. The size of the individual corrections and also the difference between the analyzed schemes varies significantly with the relevant parameters, μ, $\tan\beta$, $m_{\tilde g}$ and M_A. We estimate the uncertainty from missing higher-order corrections

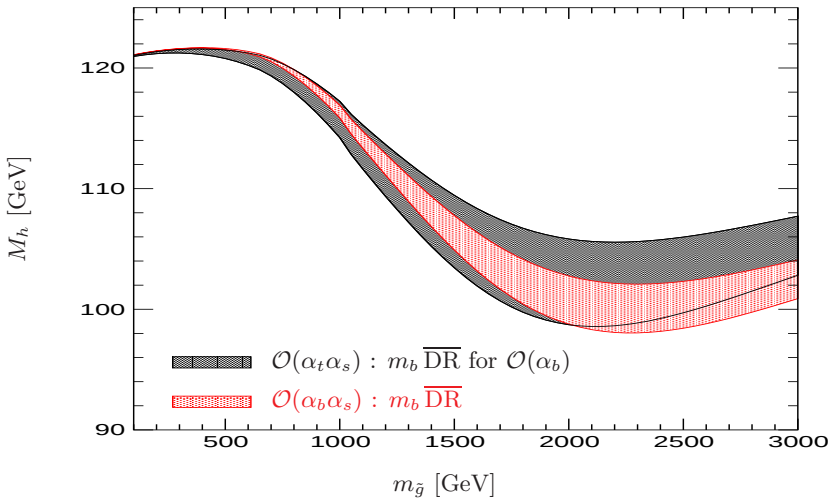

Figure 4: $\mu^{\overline{\rm DR}}$ dependence of M_h as a function of $m_{\tilde g}$. The black area corresponds to the $\mathcal{O}(\alpha_t\alpha_s)$ result including resummation, i.e. the result without the subleading two-loop $\mathcal{O}(\alpha_b\alpha_s)$ terms. The parameters are the same as in Fig. 3.

in the $b/\tilde{b}$ sector to be about 2 GeV in this region of parameter space.

The results obtained will be implemented into the Fortran code *FeynHiggs* [11, 20, 26].

References

[1] H.P. Nilles, *Phys. Rep.* **110** (1984) 1; H.E. Haber and G.L. Kane, *Phys. Rep.* **117** (1985) 75; R. Barbieri, *Riv. Nuovo Cim.* **11** (1988) 1.

[2] [LEP Higgs working group], *Phys. Lett.* **B 565** (2003) 61, hep-ex/0306033.

[3] [LEP Higgs working group], hep-ex/0107030; hep-ex/0107031; LHWG-Note 2004-01, see: `lephiggs.web.cern.ch/LEPHIGGS/papers/` .

[4] ATLAS Collaboration, *Detector and Physics Performance Technical Design Report*, CERN/LHCC/99-15 (1999), see: `atlasinfo.cern.ch/Atlas/GROUPS/PHYSICS/TDR/access.html` ;
CMS Collaboration, see: `cmsinfo.cern.ch/Welcome.html/CMSdocuments/CMSplots/` .

[5] M. Dührssen, S. Heinemeyer, H. Logan, D. Rainwater, G. Weiglein and D. Zeppenfeld, *Phys. Rev.* **D 70** (2004) 113009, hep-ph/0406323.

[6] J. Aguilar-Saavedra et al., TESLA TDR Part 3, hep-ph/0106315, see: `tesla.desy.de/tdr/` .

[7] T. Abe et al. [American Linear Collider Working Group Collaboration], hep-ex/0106056.

[8] K. Abe et al. [ACFA Linear Collider Working Group Collaboration], hep-ph/0109166.

[9] S. Heinemeyer, W. Hollik and G. Weiglein, *JHEP* **0006** (2000) 009, hep-ph/9909540.

[10] S. Heinemeyer, W. Hollik and G. Weiglein, hep-ph/0412214.

[11] G. Degrassi, S. Heinemeyer, W. Hollik, P. Slavich and G. Weiglein, *Eur. Phys. J.* **C 28** (2003) 133, hep-ph/0212020.

[12] S. Heinemeyer, hep-ph/0407244.

[13] A. Djouadi, hep-ph/0503173.

[14] A. Brignole, G. Degrassi, P. Slavich and F. Zwirner, *Nucl. Phys.* **B 643** (2002) 79, hep-ph/0206101.

[15] S. Heinemeyer, W. Hollik, H. Rzehak and G. Weiglein, to appear in *Eur. Phys. J.* **C**, hep-ph/0411114.

[16] T. Banks, *Nucl. Phys.* **B 303** (1988) 172; L. Hall, R. Rattazzi and U. Sarid, *Phys. Rev.* **D 50** (1994) 7048, hep-ph/9306309; R. Hempfling, *Phys. Rev.* **D 49** (1994) 6168; M. Carena, M. Olechowski, S. Pokorski and C. Wagner, *Nucl. Phys.* **B 426** (1994) 269, hep-ph/9402253.

[17] M. Carena, D. Garcia, U. Nierste and C. Wagner, *Nucl. Phys.* **B 577** (2000) 577, hep-ph/9912516; H. Eberl, K. Hidaka, S. Kraml, W. Majerotto and Y. Yamada, *Phys. Rev.* **D 62** (2000) 055006, hep-ph/9912463.

[18] S. Martin, *Phys. Rev.* **D 65** (2002) 116003, hep-ph/0111209; *Phys. Rev.* **D 66** (2002) 096001, hep-ph/0206136; Phys. Rev. **D 67** (2003) 095012, hep-ph/0211366; *Phys. Rev.* **D 68** 075002 (2003), hep-ph/0307101; *Phys. Rev.* **D 70** (2004) 016005, hep-ph/0312092; *Phys. Rev.* **D 71** (2005) 016012, hep-ph/0405022.

[19] J. Gunion, H. Haber, G. Kane and S. Dawson, *The Higgs Hunter's Guide*, Addison-Wesley, 1990.

[20] S. Heinemeyer, W. Hollik and G. Weiglein, *Eur. Phys. J.* **C 9** (1999) 343, hep-ph/9812472.

[21] J. Küblbeck, M. Böhm and A. Denner, *Comp. Phys. Comm.* **60** (1990) 165; T. Hahn, *Comput. Phys. Comm.* **140** (2001) 418, hep-ph/0012260; The program is available via `www.feynarts.de` .

[22] T. Hahn and C. Schappacher, *Comput. Phys. Comm.* **143** (2002) 54, hep-ph/0105349.

[23] G. Weiglein, R. Scharf and M. Böhm, *Nucl. Phys.* **B 416** (1994) 606, hep-ph/9310358; G. Weiglein, R. Mertig, R. Scharf and M. Böhm, in *New Computing Techniques in Physics Research 2*, ed. D. Perret-Gallix (World Scientific, Singapore, 1992), p. 617.

[24] W. Hollik and H. Rzehak, *Eur. Phys. J.* **C 32** (2003) 127, hep-ph/0305328.

[25] A. Djouadi, P. Gambino, S. Heinemeyer, W. Hollik, C. Jünger and G. Weiglein, *Phys. Rev. Lett.* **78** (1997) 3626, hep-ph/9612363; *Phys. Rev.* **D 57** (1998) 4179, hep-ph/9710438.

[26] S. Heinemeyer, W. Hollik and G. Weiglein, *Comp. Phys. Comm.* **124** (2000) 76, hep-ph/9812320; hep-ph/0002213; M. Frank,T. Hahn, S. Heinemeyer, W. Hollik and G. Weiglein, *in preparation*. The codes are accessible via `www.feynhiggs.de` .